Accepted Manuscript

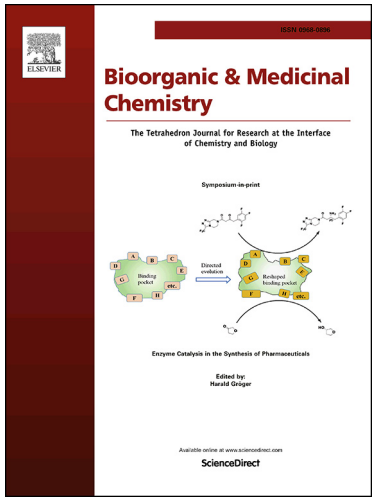

A strategic approach to the synthesis of ferrocene appended chalcone linked triazole allied organosilatranes: Antibacterial, Antifungal, Antiparasitic and Antioxidant studies

Gurjaspreet Singh, Aanchal Arora, Pooja Kalra, Indresh Kumar Maurya, Cristobal Espinosa Ruizc, M. Angeles Estebanc, Shweta Sinha, Kapil Goyal, Rakesh Sehgal

PII: S0968-0896(18)31177-5
DOI: https://doi.org/10.1016/j.bmc.2018.11.038
Reference: BMC 14642

To appear in: *Bioorganic & Medicinal Chemistry*

Received Date: 26 June 2018
Revised Date: 16 November 2018
Accepted Date: 28 November 2018

Please cite this article as: Singh, G., Arora, A., Kalra, P., Maurya, I.K., Ruizc, C.E., Estebanc, M.A., Sinha, S., Goyal, K., Sehgal, R., A strategic approach to the synthesis of ferrocene appended chalcone linked triazole allied organosilatranes: Antibacterial, Antifungal, Antiparasitic and Antioxidant studies, *Bioorganic & Medicinal Chemistry* (2018), doi: https://doi.org/10.1016/j.bmc.2018.11.038

A strategic approach to the synthesis of ferrocene appended chalcone linked triazole allied organosilatranes: Antibacterial, Antifungal, Antiparasitic and Antioxidant studies

Gurjaspreet Singh[a, *], Aanchal Arora[b, *], Pooja Kalra[a], Indresh Kumar Maurya[c], Cristobal Espinosa Ruizc[d], M. Angeles Estebanc[d], Shweta Sinha[e], Kapil Goyal[e], Rakesh Sehgal[e]

[a]Department of Chemistry and Centre of Advanced Studies, Panjab University, Chandigarh, 160014, India

[b]Department of Chemistry, Khalsa College for Women, Civil Lines, Ludhiana, 141001, India

[c]Department of Microbial Biotechnology, Panjab University, Chandigarh, 160014, India

[d]Fish Innate Immune System Group, Department of Cell Biology and Histology, Faculty of Biology, University of Murcia, 30100 Murcia, Spain

[e]Department of Medical Parasitology, Post Graduate Institute of Medical Education and Research, Chandigarh, 160024, India

[*]Corresponding Authors

1. Dr. Gurjaspreet Singh

Assistant Professor

Department of Chemistry and Centre of Advanced Studies

Panjab University, Chandigarh, India

+91-0172-2534428

Email: gjpsingh@pu.ac.in

2. Dr. Aanchal Arora

Assistant Professor

Department of Chemistry, Khalsa College for Women

Civil Lines, Ludhiana, India

+91-9530520506

Email: arora.aanchal511@gmail.com

Abstract

A series of ferrocene appended chalcone allied triazole coupled organosilatranes **(**FCTSa **7-** FCTSa **12)** were synthesised with the aim of amalgamating the pharmacological action of the constituting moieties into a single molecular scaffold. All the synthesised silatranes were well characterized by various spectroscopic techniques like IR, ^{1}H NMR, ^{13}C NMR and elemental analysis. Organosilatranes were then evaluated for their biological alacrity against bacterial and fungal strains compared with the standard drugs Rifampicin and Amphotericin B respectively. The ferrocene conjugates were found to be only moderately effective against the tested microbes. However, the organosilatranes conceded excellent efficacy against parasite *G. lamblia* with FCTSa **11** arraying the leading results. On the other hand against another parasite *T. vaginalis*, FCTSa **8** has emerged as an outstanding composite. Further, Total Antioxidant Assay (TAA) with 2,2'-azino-bis-3-(ethylbenzothiazoline-6-sulphonic acid) revealed FCTSa **10** to be the best claimant for radical scavenging activity. Along these lines, introducing some different substituents in the synthesised hybrids may act as a useful strategy for increasing the biological profile of the drugs.

Keywords: Ferrocene, Chalcone, Silatrane, Antimicrobial activity, Antiparasitic activity, Antioxidant activity

1. Introduction

Hot off the press is the molecular hybridization that has emanated as a constructive contrivance for drug design and medicinal research. This methodology inculcates the covalent linking of diverse range of pharmacophoric units into a single entity harvesting synergistic outcome [1]. The structural variations pioneered may trounce the emerging quandary of drug resistance and augment the existing drug's activity profile [2]. In consideration of this, we have contemplated the hybridisation of potentially active

functionalities autonomously playing exceptional roles in pharmaceutical industries with the aim of fabricating a conjugate with excellent effects.

Since the discovery of ferrocene, the lucrative amalgamation of classical organometallic functionality to medicinal imperative analogues has emerged as an elementary strategy towards more effective therapeutic applications [3-5]. Decoding the action mechanism of ferrocene based drugs reveal an indispensable role of this metallocenic moiety in drug action thus widening the scope of bioorganometallic chemistry for the next generation drug discovery [6]. Ferrocene-based assemblies have attracted the keen attention of researchers from many years for their inimitable physicochemical properties, crouched toxicity, remarkable stability, swift membrane permeability, reversible redox property and plethora of biological feats [7-12]. Introducing this moiety into some other potentially active modules may lead to synergic effect on individual activities.

Silatranes are the genre of cage compounds enclosing a hypervalent silicon atom with a transannular bond to nitrogen [13]. Multifarious silatrane derivatives have been synthesised in the past decades which are known for their potential pharmacological alacrity [14]. The bioactive moieties are covalently bonded to the silatranyl fragment by means of a passable linker embracing biofissionable properties. In some reports, ferrocene moiety is linked to silatranyl fragment and the resultant ferrocenylsilatranes have been reported as proficient agents that can significantly enhance the activity profile of the bioactive pharmacophores [15].

1,2,3-triazoles form an invigorating class of compounds that can act as effective linker clubbing the potentially active molecular frameworks [16]. Besides acting as linking thread, these five membered heterocyclic systems have myriad of flattering assets like high dipole moment, astonishing stability, synthetic accessibility and capability to form hydrogen bonds

with biological targets that has attracted the attention of both synthetic and medicinal chemists [17-20]. A convenient and easily accessible route of "click chemistry" for the synthesis of 1,2,3-triazoles is also accountable for their extensive use in shaping diverse structural chimeras [21].

Literature also reports the blending of ferrocene fragment to another medically budding functionality, chalcone; known for its anticancer, antioxidant, antitubercular and antiviral drug profile [22-25]. Ferrocenyl chalcones are considered as excellent targets as the derived reveries flaunt broad spectrum of lipophilic profile and versatile biological concert [26,27]. Kumar et al. have authenticated the antimalarial and antitubercular role of ferrocenyl-chalcone conjugates [28,29]. Recent revelation from our group has shown the introduction of silatranyl nucleus into the chalcone fragment, linked via 1,2,3-triazole ring with the resulting hybrids presenting a spectacular antiparasitic conduct [30].

In a quest to synthesise new hybrids with enhanced drug profile, we have designed a series of ferrocenyl hybrids following a persistent decorum of "click silylation", thus upholding the incentive of high atom economy and wide structural diversity. To the best of our knowledge, the concoction of silatranyl fragment with the potentially dynamic ferrocenyl-chalcone-triazole hybrid has been reported for the first time in this manuscript. The present work aims to exploit the structural diversity of chalcone, chemical tunability of ferrocene, incalculable stability of triazole and unique chattels of silatrane to design a family of conjugated silatranyl frameworks which are then evaluated for their antibacterial, antifungal, antiparasitic and antioxidant drug profile.

2. Results and Discussion

2.1. Drug Design

The agility of the ferrocene moiety to undergo extensive chemical modification has lead to rapid expansion in the field of ferrocene chemistry. Amendments are done in allure of synthesising substrates that mimic organic drugs and are spectacularly more effectual than the original organic pedestal. In view of this, we have designed a series of ferrocenyl chalcone linked triazole allied silatranes **7-12** following "Molecular hybridization". The synthesis was planned in such a way that the dynamic fraction of all the functionalities contributes to the ultimate hybrid producing certain kind of concerted response. Ferrocenyl chalcone derivatives can be designed by either substituting Ring A or Ring B of chalcones with a ferrocenyl fragment thus generating two series of ferrocenyl chalcones with Type 1 in which carbonyl group is directly linked to ferrocene ring while Type 2 contains carbonyl group attached to phenyl ring a shown in Fig. 1. Both categories of compounds have been synthesised and different substitutions are auditioned for the purpose of studying the Structure Activity Relationship (SAR) of the resultant compounds.

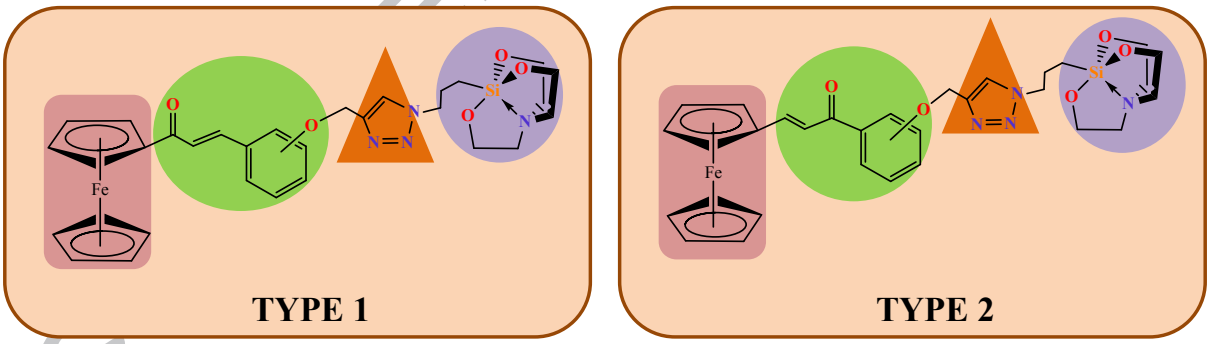

Figure 1. Type 1 and Type 2 of ferrocenyl chalcone linked triazole allied silatranes.

2.2. Chemistry

The synthetic route followed for the synthesis of four component conjugated system of ferrocene linked chalcone allied triazole encapped silatranes (FCTSa **7-12**) is summarized in Scheme 1. Isomeric compounds differ in their properties and may exhibit a completely different biological role. So, to investigate the effect of isomers, isomeric compounds were

synthesized and then compared for their biological properties to see whether the reversal of the rings joined by the conjugation bridge has any effect on their drug action or not. Acetylinic aldehydes were initially prepared by the reaction of hydroxy aldehydes with propargyl bromide in the presence of K_2CO_3 as catalyst and DMF as reaction medium. These alkyne terminated aldehydes then undergo base catalysed Claisen-Schmidt condensation with acetyl ferrocene to give ferrocene chalconyl linked acetylenes FCA. For the synthesis of isomeric FCA, aldol condensation of ferrocene 2-carboxaldehyde was done with alkyne terminated acetophenones in the presence of methanolic NaOH.

The next step involves the click reaction of FCA with AzPTES following highly efficient copper catalysed azide-alkyne cycloaddition (CuAAC) in the presence of THF/Et_3N solvent system and bromotris(triphenylphosphine)copper (I) as catalyst to give ferrocenyl chalcone linked triazole encapped organotriethoxysilanes FCTS **1-6** in good to excellent yields. In the final step, ethoxy groups of the silanes are transesterified with triethanolamine by refluxing for about 5 h in the presence of KOH as catalyst to yield corresponding ferrocene appended chalcone linked triazole encapped silatranes FCTSa **7-12** as dark red colored solid.

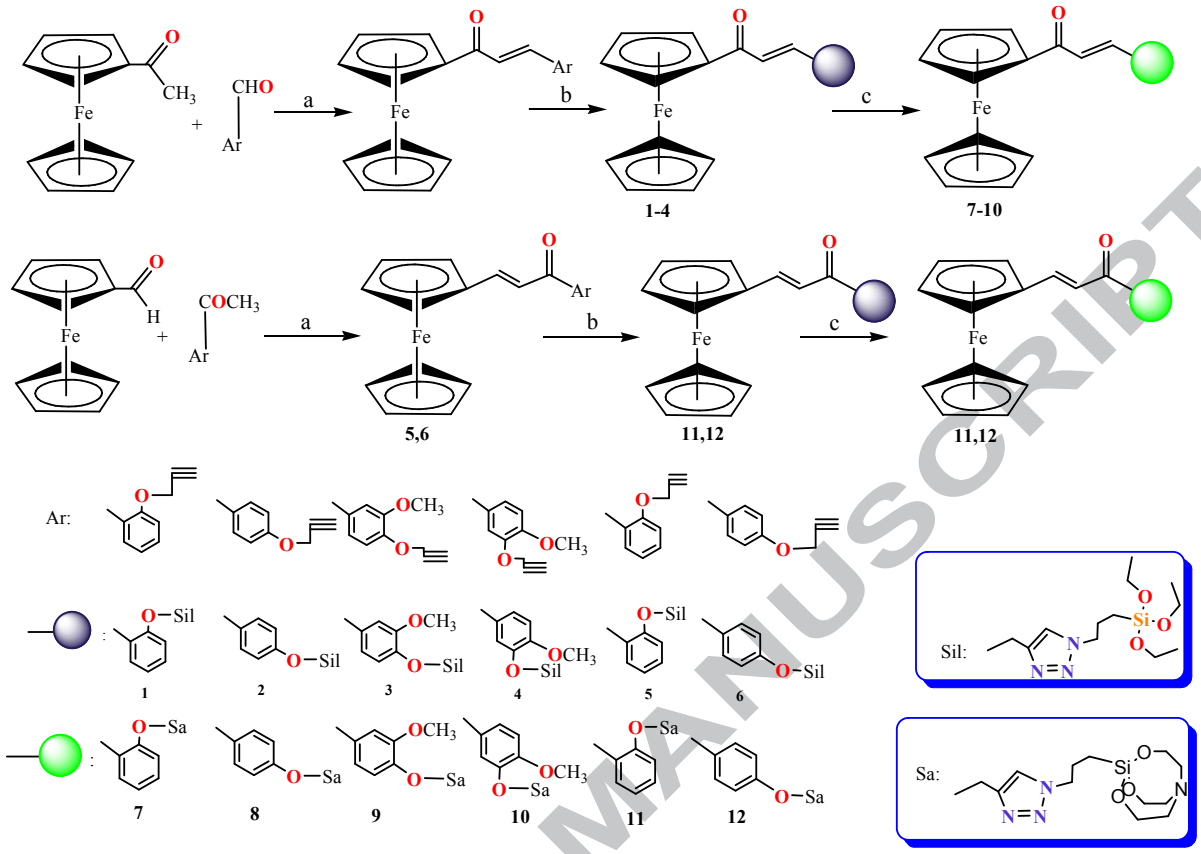

Scheme 1. Synthetic procedure for ferrocene tethered chalcone appended triazole encapped organosilatranes. *Reagents and conditions:* a) 10% NaOH, Methanol, rt, 16 h; b) AzPTES $CuBr(PPh_3)_3$, THF, Et_3N, 60 °C, 5 h; c) Triethanolamine, KOH, Toluene, 5 h reflux.

The IR spectra of the newly synthesized compounds **7-12** were recorded in the range of 4000-400 cm^{-1}. The absorption frequencies were found to be in agreement with the structure of the prepared compounds. All the compounds show absorption bands in the range of 473-483 cm^{-1}, 1235-1258 cm^{-1} and 1368-1378 cm^{-1} typical of ferrocenyl stretching vibrations and in the range of 1640-1648 cm^{-1} corresponding to C=O stretching. Stretching vibrations of C=CH of the triazole ring in the range of 2958-2973 cm^{-1} gives the evidence of cycloaddition of acetylinic unit. Furthermore, Si-O stretching vibrations appear in all the silatranes in the range of 792-799 cm^{-1} and 1074-1075 cm^{-1}. In the IR spectra of all organosilatranes,

stretching vibration corresponding to N→Si coordinate bond appears in the range of 538-540 cm^{-1}.

^{1}H NMR spectra are well consistent with the structure of the synthesized compounds. In the NMR spectra of organosilatranes **7**, two equivalent triplets appear at δ = 2.72 ppm and δ = 3.67 ppm corresponding to $-NCH_2$ and $-OCH_2$ protons respectively of $Si(OCH_2CH_2)_3N$ skeleton. These signals of $-NCH_2$ and $-OCH_2$ protons were observed at δ = 2.74 ppm and 3.68 ppm, 2.51 ppm and 3.75 ppm, 2.69 ppm and 3.63 ppm, 2.74 ppm and 3.68 ppm, 2.73 ppm and 3.68 ppm for organosilatranes **8-12** respectively. Additionally, presence of a signal around δ = 7.60 ppm, 7.67 ppm, 7.45 ppm, 7.55 ppm, 7.48 ppm and 7.40 ppm for organosilatranes **7-12** respectively validates the presence of a triazole proton. Furthermore, absence of a triplet around δ = 1.2 ppm and quartet around δ = 3.7 ppm affirms the complete esterification of the silyl group into silatranyl fragment. Parallel shifting is scrutinized in the carbon spectra of the respective compounds. The highly shielded protons are the ones attached to the carbon directly linked to silicon appearing at δ = 12.9 ppm, 13.7 ppm, 13.4 ppm, 13.2 ppm, 13.0 ppm and 12.2 ppm for organosilatranes **7-12** respectively.

The carbonyl carbon appears as the least shielded carbon in the spectrum at δ = 189.0-193.1 ppm. In ^{13}C NMR spectra of the organosilatranes, the ferrocenyl carbons appear around δ = 68.8-80.8 ppm in all the compounds **7-12**. The vinylic carbons of the chalcone functionality appear at 124.0-129.9 ppm and 134.1-139.5 ppm. In ferrocene linked organosilatranes **7-12**, the peaks at δ = 49.8-51.5 ppm and δ = 56.0-56.6 ppm are assigned to $-NCH_2$ and $-OCH_2$ carbons of silatranyl moiety. Moreover, absence of signals around δ = 18.0 ppm and 58.0 ppm corresponding to CH_3 and $OCH_2\mathbf{C}H_3$ carbons of the ethoxy groups of the silanes affirms the complete esterification of the silanes. Carbon attached to silicon appears as the most shielded carbon at δ = 12.2-13.7 ppm clearly indicating the hypervalency in the final

compounds. Additionally, carbons of the triazole ring emerging at δ = 119.9-122.9 ppm and δ = 135.2-141.6 ppm clearly mark the presence of triazole assembly.

2.3. Computational Analysis

Traditional clinical methods involve multi-step time consuming drug testing against a series of biological screens that may sometimes lead to adverse findings ultimately resulting into haltering of the project to find some other clinical candidate. This deplorable burden on the research and development may be overcome by prior computational screening of the designed compounds. The high throughput screening of the synthesised library reduces the risk of late stage debilitation of the tested compounds. Pharmacokinetics parameters like absorption, distribution, metabolism, excretion and toxicity are therefore tested using computer based ADMET predictor. All these properties have been listed in Table 1.

First step is the absorption of drugs for which a drug must be orally bio available and after reaching the gastro-intestinal tract, drugs must be able to surpass the biological membranes to enter the systemic circulation. This process depends on parameters like permeability and compound solubility. So, the permeation of the drugs is being assayed here using artificial membrane assays such as Caco-2 and MDCK cell lines. Results reveal that chalcone appended ferrocenyl silatranes offer moderate permeability through both the cell lines. Solubility in the intestinal fluid is also considered as a significant asset of any oral drug as the inadequate solubility may hinder its intestinal absorption through the hepatic portal system. Next is the penetration of the drugs that have to enter into the central nervous system for which they must primarily cross the blood brain barrier (BBB) through either active transport or by passive diffusion. However, for non-CNS drugs, BBB penetration must be minimized to reduce the risk of detrimental pharmacological actions

and possible neurotoxicity. Another important parameter is Plasma Protein Binding (PPB). As only the unbound drug can cross membranes and interact with the protein target, so interaction with plasma proteins must be vigilantly monitored during the drug discovery process.

Further parameters like Human Intestinal Absorption (HIA) and Skin Permeability identifies the potential drug for oral and transdermal delivery. HIA describes the percentage of orally administered drug reaching the hepatic portal vein and our computational analysis has shown a high value of HIA for all the synthesised compounds. Skin Permeability is analysed from the permeability coefficient data (K_p) that provides an imperative insight into the molecular transport through the stratum corneum.

$$K_p = K_m * D/h$$

where K_m is distribution coefficient between stratum corneum and vehicle, D is average diffusion coefficient (cm^2/h) and h is thickness of skin (cm). All these assays together can significantly assist the selection of potential drug candidates with enhanced probability of clinical success.

Table 1. Pharmacokinetic descriptors of FCTSa **7-12**.

Descriptors / Organo silatranes	Caco-2 cell permeability (nm/s)	Buffer solubility (mg/l)	BBB	HIA (%)	MDCK (nm/s)	Plasma protein binding (%)	Skin permeability ($logK_p$)
7	33.52	1304.91	2.59	97.79	0.025	100.00	-4.91
8	31.68	2329.01	2.59	97.79	0.037	100.00	-4.91
9	31.34	1265.37	2.10	97.74	0.024	100.00	-4.93
10	31.40	1265.37	2.10	97.74	0.024	100.00	-4.93
11	33.39	652.10	2.83	97.79	0.030	100.00	-4.90
12	31.37	1163.86	2.83	97.79	0.034	100.00	-4.90

BBB: Blood Brain Barrier; HIA: Human Intestinal Absorption; MDCK: Madin-Darby Canine Kidney

2.4. Biological Assays

Ferrocene moiety is extensively known for its pharmacological implication. In the synthesized motifs, besides ferrocene, there are three auxiliary bioactive functionalities, that is chalcone, 1,2,3-triazole and silatrane. All these vibrant clusters have been clubbed together with a motive to augment their pharmaceutical action. To have a look into their synergistic effect, ferrocenyl silatranes FTCSa **7-12** were evaluated for their antimicrobial activities against several strains of bacteria and fungi, antiparasitic activities against *G. lamblia* and *T. vaginalis* and antioxidant assays.

2.4.1. In vitro anti-microbial activity

Microbial infections are posing a serious threat to public health worldwide accounting for around 50,000 deaths each day [31]. The progressively increasing multidrug resistance to the existing drugs is totting up the concern of medicinal chemists. This has led to the abundant structural and chemical modifications in the recognized drugs to give rise to a new generation of antimicrobials that can combat the emergence of multidrug resistance [32]. In view of this, the synthesised multicomponent motifs were evaluated against six strains of bacteria and seven strains of fungi and compared with the standard drugs Rifampicin and Amphotericin B respectively. The subsequent antibacterial and antifungal results are detailed in Table 2 and 3 respectively. It is worth mentioning that despite their moderate activity, synthesised silatranes were found to be effective against all the tested bacterial strains. However, these were comparatively more vigorous against numerous strains of fungi. This observation entails that the assembled unit provides a broad spectrum of antibacterial and antifungal conduct, though further research is required to improve their activity profile. So, auxiliary structural modifications like the introduction of new substituents at the chalcone or the ferrocene ring that can enhance their microbial potency is our ongoing topic of research.

Among the evaluated bacterial strains, *L. monocytogens* was the most resistant one to ferrocenyl derivatives. In contrast, the best potency was shown against *E. faecalis* strain of

bacteria. FCTSa **9** was the most effective derivative against the bacterial strains. As a general view, ortho derivatives were more active than the ones in which silatrane is present at the para position. Considering fungal strains, *C. albicans* was the most affected while *C. kusei* was the least bothered fungal strain. FCTSa **10** was found to be most effective against *C. albicans* while FCTSa **8** displayed the highest activity against *C. tropicalis* fungi both divulging the IC_{50} value of 31.25 µM. Amongst all silatranes, FCTSa 7 was the most potent compound against all strains of fungi. Further optimizations on this structural outfit may eventually lead to the innovation of more potential therapeutic agents.

Table 2. Antibacterial activity of silatranes **7-12** (IC_{50} values in µM).

FCTSa	*E. coli*	*S. aureus*	*E. faecalis*	*V. cholera*	*H.influenza*	*L. monocytogens*
7	250	125	>250	125	>250	250
8	250	250	>250	>250	>250	>250
9	125	250	125	>250	125	250
10	250	>250	125	>250	125	>250
11	n.d.	n.d.	n.d.	n.d.	n.d.	n.d.
12	125	>250	125	>250	>250	>250
Rifampicin	7.60	1.90	62.50	62.50	62.50	125

*n.d.: Not determined due to solubility reasons

Table 3. Antifungal activity of silatranes **7-12** (IC_{50} values in µM).

FCTSa	*C. kusei*	*C. albicans*	*C. tropicalis*	*C. parapsolsis*	*C. kyfer*	*C. neoformans*	*C. glabrata*
7	250	125	125	62.50	62.50	62.50	125
8	>250	62.50	31.25	>250	>250	>250	>250
9	>250	62.50	>250	>250	>250	>250	>250
10	>250	31.25	>250	>250	>250	>250	>250
11	n.d.	n.d.	n.d.	n.d.	n.d.	n.d.	n.d.
12	>250	125	125	>250	>250	>250	>250

Amphotericin B	0.78	0.78	0.78	0.78	1.25	0.195	0.78

*n.d.: Not determined due to solubility reasons

2.4.2. Antiparasitic Assay

Parasitic diseases are causing a serious health dilemma affecting both plants and animals. Of these, giardiasis caused by protozoan parasite *G. lamblia* is the most important one distressing around 280 million people, especially children, around the world [33]. Giardiasis is often manifested by clinical symptoms like malabsorption, diarrohea, abdominal pain, nausea and negative impact on overall growth and development [34]. Another important parasitic disease is trichomoniasis caused by the flagellated protozoan parasite *T. vaginalis*. Sexually transmitted diseases caused by this parasite are long been posing a serious threat to mankind affecting nearly 340 million people every year [35]. Trichomoniasis infected patients are posed to serious threats of cervical cancer and HIV transmission [36]. The existing drugs either show low efficacy or are associated with adverse effects and are often coupled with augmentation of resistant strains thus prompting efforts to develop new therapeutics [37].

Consequently, organosilatranes FCTSa **7-12** were assayed against *G. lamblia* and *T. vaginalis* and the results revealed that all the organosilatranes exhibited higher potency against *G. lamblia* compared to *T. vaginalis* with IC_{50} values ranging from 0.57-113.8 µM against giardial parasites. FCTSa **11** was the most promising candidate displaying the phenomenal activity against *G. lamblia* on the exposure of parasites for 24 h while increasing this time to 48 h, FCTSa **7** exhibited best response against this parasite. In general, FCTSa **8** presented good potency against both the parasites. Biological assay results against *T. vaginalis* showed that most of the compounds exhibited comparatively low bioactivity with IC_{50} ranging from

22.90-116.9 µM. FCTSa **10** was the least effective organosilatrane against both the parasites and at both time points.

Table 4. Antiparasitic activity of silatranes **7-12**.

Compounds	*G. lamblia*		*T. vaginalis*	
	IC_{50} (µM) 24 h	IC_{50} (µM) 48 h	IC_{50} (µM) 24 h	IC_{50} (µM) 48 h
7	113.8	1.57	115.7	38.81
8	6.27	10.89	57.72	22.90
9	17.77	9.18	82.65	n.d.
10	n.d.	130	116.9	81.74
11	0.57	n.d.	68.10	n.d.
12	87.04	4.25	102.2	n.d.

*n.d.: Not determined due to solubility reasons

2.4.3. Antioxidant Assay

The antioxidant effect can be estimated from the ability to scavenge radicals and inhibit oxidation of biological species [38]. As literature reports, radical scavenging efficacy of ferrocenyl chalcones is higher than the chalcone itself [39], so synthesised ferrocenyl chalcones are investigated for their antioxidant activity in aid of which stable radical like ABTS is used to test the ability of an antioxidant to reduce radicals. The redox action of Fe(II)/Fe(III) present in ferrocene moiety counts for its abundant antioxidant activity [40]. The Total Antioxidant Activity (TAA) results revealed FCTSa **10** to show the best activity among all the silatranes while FCTSa **9** was the least effective one.

Table 5. Total Antioxidant Activity expressed in equivalents of ascorbic acid (mM) per mg of the compounds (7-12).

S. No.	TAA (eq.asc) mM mg NP
7	7.4±1.5
8	10.3±0.8
9	23.0±0.5
10	5.00±0.07
11	n.d.
12	15.8±0.3

*n.d.: Not determined due to solubility reasons

3. Experimental

3.1. Chemistry

3.1.1. Starting Material

Propargyl bromide (80% in toluene) (Aldrich), o/p-hydroxyacetophenones (AVRA), potassium carbonate (Thomas), sodium hydroxide (LOBA Chemie), sodium sulphate (Finar), sodium azide (AVRA), 3-chloropropyltriethoxysilane (Aldrich), Bromotris(triphenylphosphine)copper(I) [$CuBr(PPh_3)_3$] (Aldrich), triethanolamine (LOBA Chemie), potassium hydroxide (Finar) were used as received. The organic solvents were dried according to standard procedures. 3-azidopropyltriethoxysilane (3-AzPTES) was synthesized from 3-chloropropyltriethoxysilane by known procedure from literature (SI) [41].

3.1.2. Measurements

Infrared spectrum was obtained as Neat on a Thermo Scientific Fischer spectrometer. The NMR spectra (^1H and ^{13}C) were recorded on a JEOL (AL 300 MHz) and BRUKER (400 MHz) spectrometer using $CDCl_3$ as internal reference and chemical shifts were reported relative to tetramethylsilane. *J* values are given in Hz. The following abbreviations are used: s, singlet; d, doublet; q, quartet; t, triplet; m, multiplet. Melting points were measured in a Mel Temp II device using sealed capillaries and were uncorrected. CHN analysis was

obtained on Perkin Elmer Model 2400 CHNS elemental analyzer and Thermo Scientific Flash 2000 organic elemental analyzer. Mass spectral measurements (TOF MS ESþ 1.38 eV) were carried out on Waters Q–TOF Micro Mass Spectrometer. Column chromatography was performed with E. Merck silica gel (Kieselgel 60, 230-400 mesh). Analytical thin layer chromatography was performed employing 0.2 mm coated commercial silica gel plates (E. Merck, DC-Aluminium sheets, Kieselgel 60 F254).

3.1.3. General procedure for the synthesis of ferrocenyl chalcone appended triazole allied triethoxysilanes **(1-6)**

Acetylinic ferrocene appended chalcones were synthesised following literature reports [42]. (1.0 equiv) of this acetylene was added to 1:1 THF/Et_3N solvent mixture taken in a two-neck round bottomed flask and the mixture was stirred for 15 min at room temperature. Then, slow addition of AzPTES (1.0 equiv) was done followed by catalyst [$CuBr(PPh_3)_3$] (0.01 mmol) loading and the mixture was stirred at 60 °C for 8-10 h. The reaction was then brought to room temperature. The solvents were evaporated under reduced pressure followed by the addition of hexane. The reaction mixture was then filtered and concentration of filtrate under reduced pressure afforded the viscous red silane in excellent yield (82 to 94%). The characterization data of all the synthesised silanes was found to be as per the literature upholdings [42].

3.1.4. General procedure for the synthesis of ferrocenyl chalcone appended triazole allied organosilatranes **(7-12)**

1 equiv of organotriethoxysilane (**1-6)** is taken in a two necked round bottomed flask fitted with a Dean-Stark assembly followed by the addition of 20 ml toluene, 1 equiv of triethanolamine and catalytic amount of KOH. The reaction mixture was then refluxed for 4 h. Thereafter, the solvent was evaporated under vacuum and on slow addition of hexane (10 ml), solid precipitated out. The solid so obtained was left for overnight stirring and then

filtered under nitrogen and dried under vacuum resulting into desired organosilatranes **7-12** in excellent yields. The structures of the synthesised hybrids have been detailed in Table 6.

3.1.4.1. Synthesis of (E)-1-(ferrocenyl)-3-(2-((1-(3-(silatranyl)propyl)-1H-1,2,3-triazol-4-yl)methoxy)-phenyl)prop-2-en-1-one **(7):** The quantities used were as: **1** (1.00 g, 1.62 mmol), triethanolamine (0.24 g, 1.62 mmol). Dark red solid, Yield: 0.90 g, 89 %. M.P.: Charring at 110 °C. Anal. Calcd. for $C_{31}H_{36}FeN_4O_5Si$: C, 59.23; H, 5.77; N, 8.91. Found: C, 59.19; H, 5.71; N, 8.84. IR (neat, cm^{-1}): 482 (Fe-Cp), 538 (N→Si), 798, 1075 (Si-O), 1235, 1376 (CpC=C), 1646 (C=O), 2968 (C=C-H). ^{1}H NMR (300 MHz, $CDCl_3$, 25 °C): δ 0.37 (s, 2H, -$SiCH_2$-), 1.96 (s, 2H, -CCH_2C-), 2.72 (s, 6H, -CH_2N-), 3.67 (s, 6H, -OCH_2-), 4.09 (s, 5H, FcH), 4.30 (s, 2H, -N_3CH_2-), 4.47 (s, 2H, FcH), 4.69 (s, 2H, FcH), 5.25 (s, 2H, -OCH_2-), 6.95-7.08 (m, 2H, H2, H4), 7.40-7.51 (m, 3H, Hα, H3, H5), 7.60 (s, 1H, Tz-H), 7.89 (d, J = 15.7 Hz, 1H, Hβ). ^{13}C NMR (101 MHz, $CDCl_3$): δ = 12.9 ($SiCH_2$), 26.1 (C**C**H_2C), 49.9 (CH_2**C**H_2N), 53.4 (N_3CH_2), 56.5 (O**C**H_2CH_2), 61.3 (OCH_2), 69.1, 69.9, 71.6, 80.5 (Fc-C), 113.2 (C3), 116.8 (C5), 122.3, 141.6 (Tz-C), 124.9 (Cα), 127.5 (C1), 131.0 (C4), 131.1 (C6), 135.4 (Cβ), 157.8 (C2), 192.5 (C=O). MS: m/z 629 $[M + H]^+$.

3.1.4.2. Synthesis of (E)-1-(ferrocenyl)-3-(4-((1-(3-(silatranyl)propyl)-1H-1,2,3-triazol-4-yl)methoxy)-phenyl) prop-2-en-1-one **(8):** The quantities used were as: **2** (1.00 g, 1.62 mmol), triethanolamine (0.24 g, 1.62 mmol). Dark red solid, Yield: 0.88 g, 87 %. M.P.: Charring at 180 °C. Anal. Calcd. for $C_{31}H_{36}FeN_4O_5Si$: C, 59.23; H, 5.77; N, 8.91. Found: C, 59.16; H, 5.69; N, 8.87. IR (neat, cm^{-1}): 482 (Fe-Cp), 538 (N→Si), 796, 1074 (Si-O), 1254, 1377 (CpC=C), 1648 (C=O), 2973 (C=C-H). ^{1}H NMR (300 MHz, $CDCl_3$, 25 °C): δ 0.35 (s, 2H, -$SiCH_2$-), 1.92 (s, 2H, -CCH_2C-), 2.74 (s, 6H, -CH_2N-), 3.68 (s, 6H, -OCH_2-), 4.14 (s, 5H, FcH), 4.51 (s, 2H, -N_3CH_2-), 4.68 (s, 2H, FcH), 4.83 (s, 2H, FcH), 5.17 (s, 2H, -OCH_2-), 6.96 (s, 2H, H2, H6), 7.40 (s, 1H, Hα), 7.54 (s, 2H, H3, H5), 7.67 (s, 2H, Tz-H, Hβ). ^{13}C NMR (101 MHz, $CDCl_3$): δ = 13.7 ($SiCH_2$), 26.2 (C**C**H_2C), 51.5 (CH_2**C**H_2N), 53.0 (N_3CH_2),

56.6 (O**C**H_2CH_2), 61.1 (OCH_2), 69.7, 70.1, 72.7, 80.7 (Fc-C), 115.3 (C3, C5), 122.9, 135.2 (Tz-C), 129.9 (Cα), 131.5 (C2, C6), 132.2 (C1), 136.1 (Cβ), 163.3 (C4), 189.7 (C=O).

Synthesis of (E)-1-(ferrocenyl)-3-(4-((1-(3-(silatranyl)propyl)-1H-1,2,3-triazol-4-yl)methoxy)-3-methoxyphenyl)prop-2-en-1-one **(9):** The quantities used were as: **3** (1.00 g, 1.54 mmol), triethanolamine (0.23 g, 1.54 mmol). Dark red solid, Yield: 0.84 g, 83 %. M.P.: Charring at 136 °C. Anal. Calcd. for $C_{32}H_{38}FeN_4O_6Si$: C, 58.36; H, 5.82; N, 8.51. Found: C, 58.27; H, 5.81; N, 8.46. IR (neat, cm^{-1}): 483 (Fe-Cp), 540 (N→Si), 796, 1074 (Si-O), 1254, 1378 (CpC=C), 1644 (C=O), 3072 (C=C-H). ^{1}H NMR (300 MHz, $CDCl_3$, 25 °C): δ 0.42 (s, 2H, -$SiCH_2$-), 1.97 (s, 2H, -CCH_2C-), 2.51 (s, 6H, -CH_2N-), 3.75 (s, 6H, -OCH_2-), 3.97 (s, 3H, -OCH_3), 4.21 (s, 5H, FcH), 4.58 (s, 2H, -N_3CH_2-), 4.83 (s, 2H, FcH), 4.92 (s, 2H, FcH), 5.25 (s, 2H, -OCH_2-), 7.00 (s, 2H, Hα, H5), 7.10-7.16 (m, 2H, H2, H6), 7.46 (s, 1H, Tz-H), 7.71 (d, *J* = 15.7 Hz, 1H, Hβ). ^{13}C NMR (101 MHz, $CDCl_3$): δ = 13.4 ($SiCH_2$), 27.4 (C**C**H_2C), 49.8 (CH_2**C**H_2N), 53.7 (N_3CH_2), 56.1 (O**C**H_2CH_2), 56.7 (OCH_3), 60.8 (OCH_2), 69.7, 70.1, 72.7, 80.7 (Fc-C), 111.2 (C2), 113.9 (C5), 121.5 (C1), 121.8 (C6), 122.2, 140.8 (Tz-C), 124.0 (Cα), 134.2 (Cβ), 148.6 (C4), 151.8 (C3), 193.0 (C=O). MS: m/z 659 $[M + H]^+$.

3.1.4.3. Synthesis of (E)-1-(ferrocenyl)-3-(3-((1-(3-(silatranyl)propyl)-1H-1,2,3-triazol-4-yl)methoxy)-4-methoxyphenyl)prop-2-en-1-one **(10):** The quantities used were as: **4** (1.0 g, 1.54 mmol), triethanolamine (0.23 g, 1.54 mmol). Dark red solid, Yield: 0.85 g, 84 %. M.P.: Charring at 122 °C. Anal. Calcd. for $C_{32}H_{38}FeN_4O_6Si$: C, 58.36; H, 5.82; N, 8.51. Found: C, 58.25; H, 5.76; N, 8.43. IR (neat, cm^{-1}): 473 (Fe-Cp), 539 (N→Si), 797, 1074 (Si-O), 1258, 1376 (CpC=C), 1645 (C=O), 2961 (C=C-H). ^{1}H NMR (300 MHz, $CDCl_3$, 25 °C): δ 0.30 (s, 2H, -$SiCH_2$-), 1.90 (s, 2H, -CCH_2C-), 2.69 (s, 6H, -CH_2N-), 3.63 (s, 6H, -OCH_2-), 3.85 (s, 3H, -OCH_3), 4.16 (s, 5H, FcH), 4.25 (s, 2H, -N_3CH_2-), 4.48 (s, 2H, FcH), 4.89 (s, 2H, FcH), 5.23 (s, 2H, -OCH_2-), 7.05-7.12 (m, 3H, Hα, H2, H3), 7.25 (s, 1H, H6), 7.55-7.62 (m,

2H, Tz-H, Hβ). ^{13}C NMR (75 MHz, $CDCl_3$): δ = 13.2 ($SiCH_2$), 26.4 ($C\mathbf{C}H_2C$), 51.0 ($CH_2\mathbf{C}H_2N$), 53.5 (N_3CH_2), 56.0 ($O\mathbf{C}H_2CH_2$), 57.6 (OCH_3), 61.8 (OCH_2), 69.8, 70.2, 72.8, 80.8 (Fc-C), 111.4 (C2), 117.1 (C5), 119.9, 140.7 (Tz-C), 121.3 (C1), 123.2 (C6), 128.6 (Cα), 134.1 (Cβ), 148.0 (C3), 152.9 (C4), 193.1 (C=O).

3.1.4.4. Synthesis of (E)-3-(ferrocenyl)-1-(2-((1-(3-(silatranyl)propyl)-1H-1,2,3-triazol-4-yl)methoxy)-phenyl)prop-2-en-1-one **(11):** The quantities used were as: **5** (1.00 g, 1.62 mmol), triethanolamine (0.24 g, 1.62 mmol). Yellow solid, Yield: 0.84 g, 83 %. M.P.: Charring at 128 °C Anal. Calcd. for $C_{31}H_{36}FeN_4O_5Si$: C, 59.23; H, 5.77; N, 8.91. Found: C, 59.17; H, 5.68; N, 8.83. IR (neat, cm^{-1}): 479 (Fe-Cp), 539 (N→Si), 792, 1074 (Si-O), 1256, 1376 (CpC=C), 1648 (C=O), 2958 (C=C-H). ^{1}H NMR (300 MHz, $CDCl_3$, 25 °C): δ 0.38 (s, 2H, -$SiCH_2$-), 1.97 (s, 2H, -CCH_2C-), 2.74 (s, 6H, -CH_2N-), 3.68 (s, 6H, -OCH_2-), 4.10 (s, 5H, FcH), 4.30 (s, 2H, -N_3CH_2-), 4.48 (s, 2H, FcH), 4.70 (s, 2H, FcH), 5.25 (s, 2H, -OCH_2-), 6.98-7.07 (m, 2H, H3, H5), 7.41 (s, 2H, Hα, H4), 7.48 (s, 1H, Tz-H), 7.60 (s, 2H, H6, Hβ). ^{13}C NMR (101 MHz, $CDCl_3$): δ = 13.0 ($SiCH_2$), 26.0 ($C\mathbf{C}H_2C$), 51.1 ($CH_2\mathbf{C}H_2N$), 53.1 (N_3CH_2), 56.6 ($O\mathbf{C}H_2CH_2$), 61.4 (OCH_2), 69.7, 70.1, 72.7, 80.7 (Fc-C), 115.9 (C3), 121.8 (C5), 122.2, 140.8 (Tz-C), 125.8 (Cα), 128.6 (C6), 129.3 (C1), 135.6 (C4), 136.8 (Cβ), 161.2 (C2), 191.4 (C=O).

3.1.4.5. Synthesis of (E)-3-(ferrocenyl)-1-(4-((1-(3-(silatranyl)propyl)-1H-1,2,3-triazol-4-yl)methoxy)-phenyl)prop-2-en-1-one **(12):** The quantities used were as: **6** (1.00 g, 1.62 mmol), triethanolamine (0.24 g, 1.62 mmol). Yellow solid, Yield: 0.86 g, 85 %. M.P.: 138 °C. Anal. Calcd. for $C_{31}H_{36}FeN_4O_5Si$: C, 59.23; H, 5.77; N, 8.91. Found: C, 59.19; H, 5.65; N, 8.84. IR (neat, cm^{-1}): 479 (Fe-Cp), 538 (N→Si), 799, 1075 (Si-O), 1257, 1368 (CpC=C), 1640 (C=O), 2960 (C=C-H). ^{1}H NMR (300 MHz, $CDCl_3$, 25 °C): δ 0.38 (s, 2H, -$SiCH_2$-), 1.97 (s, 2H, -CCH_2C-), 2.73 (s, 6H, -CH_2N-), 3.68 (s, 6H, -OCH_2-), 4.10 (s, 5H, FcH), 4.30 (s, 2H, -N_3CH_2-), 4.48 (s, 2H, FcH), 4.70 (s, 2H, FcH), 5.25 (s, 2H, -OCH_2-), 6.96

-7.06 (m, 2H, H3, H5), 7.40 (s, 1H, Tz-H), 7.48 (s, 1H, Hα), 7.60 (s, 2H, H2, H6), 7.93 (s, 1H, Hβ). ^{13}C NMR (101 MHz, $CDCl_3$): δ = 12.2 ($SiCH_2$), 25.3 (CCH_2C), 50.0 (CH_2CH_2N), 52.5 (N_3CH_2), 56.5 (OCH_2CH_2), 61.3 (OCH_2), 68.8, 69.1, 71.8, 79.6 (Fc-C), 115.4 (C3, C5), 122.4, 136.6 (Tz-C), 127.6 (Cα), 131.0 (C2, C6), 131.1 (C1), 139.5 (Cβ), 162.4 (C4), 189.0 (C=O).

Table 6. List of ferrocene appended chalcone linked orgnaosilatranes.

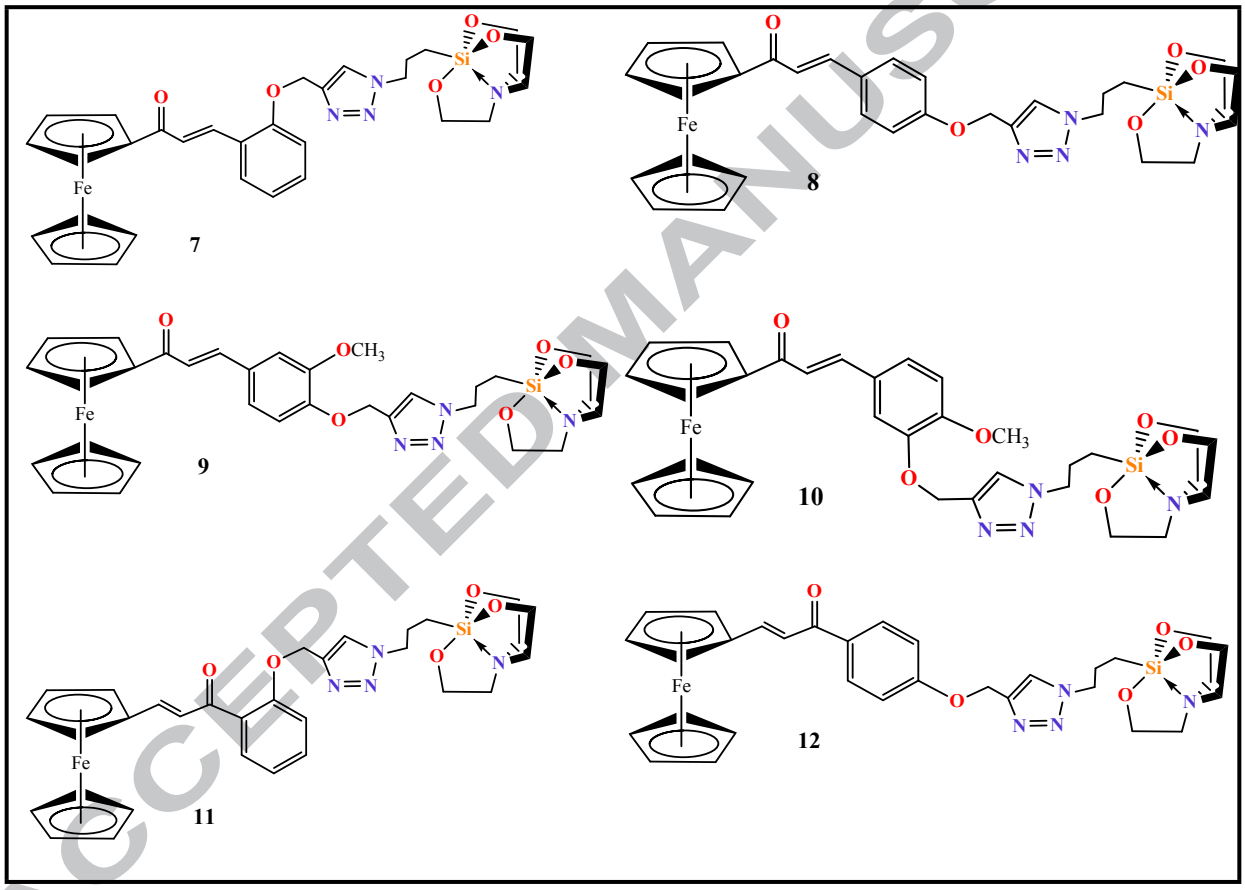

3.2. Biological Assays

3.2.1. Antiparasitic Assay

The *Giardia lamblia* strain Portland 1 (Pl) and Trichomonas vaginalis 413 strain was maintained axenically on Diamond's modified TYI-S-33 medium by incubating it at 37 °C. Drug sensitivity was performed by using MTT (3-(4,5-Dimethylthiazol-2-yl)-2,5-

diphenyltetrazolium bromide, a tetrazole) assay for all Compounds. The highest drug concentration in each row was 100 µg /ml and then doubling dilutions of the drug were performed. The plates were incubated at 37 °C for 24 h and 48 h. Following incubation at 37 °C for 24 h and 48 h, the optical density (OD) was measured in an ELISA recorder at 570 nm. IC_{50} value was calculated using Graph Pad Prism version 6.

3.2.2. Antibacterial and Antifungal Assay

The bacterial and fungal strains used in the study were procured from National Collection of Pathogenic Fungi (NCPF), Post Graduate Institute of Medical Education and Research (PGIMER), Chandigarh and Institute of Microbial Technology (MTCC-IMTECH), Chandigarh. Human embryonic kidney cells (Hek-293) were obtained from American type culture collection (ATCC-CRL1573). The pathogenic bacterial strains *Escherichia coli* (*E. coli*) MTCC2961*, Staphylococcus aureus* (*S. aureus*) MTCC3160, *Enterococcus faecalis* (*E. faecalis*) MTCC 439, *Vibrio cholera* (*V. cholera*) MTCC 3906, *Streptococcus pyogenes* (*S. pyogens*) MTCC 442*, Listeria monocytogens* (*L. monocytogens*) MTCC839 were cultured in Muller Hinton broth (MHB, HiMedia, India). The pathogenic fungal strains *Candida albican*s (*C. albicans*) NCPF400034*, Candida glabrata* (*C. glabrata*) MTCC3019, *Candida krusei* (*C. krusei*) NCPF44002, *Candida parapsilosis* (*C. parapsilosis*) NCPF450002*, Candida keyfer* (*C. keyfer*) NPCPF410004*, Candida tropicalis* (*C. tropicalis*) NPCPF420007*, Cryptococcus neoformans* (*C. neoformans*) NCPF250316 were cultured in Yeast Extract-Peptone-Dextrose (YEPD broth, HiMedia, India) and RPMI 1640 media (HiMedia, India). For agar plates, bacteriological agar (2.5% w/v, HiMedia, India) was added to the medium. The strains were stored with glycerol (15%) at -80 °C as frozen stocks. The cells were freshly revived on respective agar plates from the stock before each experiment.

3.2.3. Total Antioxidant Activity (TAA)

TAA was measured in particles using the method of Arnao, Cano and Acosta [43], which is based on the ability of the antioxidants in the sample to reduce the radical cation of 2,2'-azino-bis-3-(ethylbenzothiazoline-6-sulphonic acid) (ABTS), determined by the decolouration of $ABTS^{\cdot+}$, and measuring the quenching of the absorbance at 730 nm. The number of single electron in ABTS trapped by anantioxidant can be estimated by means of chemical kinetics [44]. Furthermore, some new ferrocenylbase are described as novel antioxidant to protect DNA against oxidation damage [45]. To do the assay, a solution containing ABTS 2 mM, horseradish peroxidase 0.25 μM and H_2O_2 35 μM was prepared. The particles were dissolved in PBS 50 mM pH= 7.5 and 50 μL of the suspension, containing 1 mg 100 μL^{-1} was added to 950 μL of the ABTS solution. The change of absorbance was followed at 730 nm for five minutes. This activity is calculated by comparing the values of the sample with a standard curve of ascorbic acid and expressed as ascorbic acid equivalents (mmol) per milligram of particle. All the samples were measured per triplicate.

4. Conclusion

The idea of inculcating the active functionality of contrasting agglomerates in a single chemical coliseum has lead to the revelation of hybrids with broad spectrum of activity profile. The synthesised ferrocene conjoined chalcone appended triazole linked organosilatranes were although only passably active against a range of bacterial and fungal strains but have shown admirable response against precarious giardial and trichomonal parasites. Ancillary to this is the antioxidant assay that has professed the tested compounds to array excellent radical scavenging efficacy. Further, peculiar substitutions may be trialled to augment the biological portrayal of the synthesised composites.

Acknowledgements

Aanchal Arora would like to thank CSIR, New Delhi for providing financial support (in the form of Junior and Senior Research Fellowships). Special thanks to Mr. Avtar Singh, SAIF, Panjab University, Chandigarh for NMR studies.

References

1. C. Viegas-Junior, A. Danuello, V. da Silva Bolzani, E.J. Barreiro, C.A.M. Fraga, Curr. Med. Chem. 14 (2007) 1829–1852.
2. M.L. Cohen, Science 257 (1992) 1050–1055.
3. C. Ornelas, New J. Chem. 35 (2011) 1973–1985.
4. F. Asghar, A. Badshah, B. Lal, S. Zubair, S. Fatima, I.S. Butler, Bioorg. Chem. 72 (2017) 215–227.
5. A. Singh, C. Biot, A. Viljoen, C. Dupont, L. Kremer, K. Kumar, V. Kumar, Chem. Biol. Drug Des. 89 (2017) 856–861.
6. L. Tabrizi, H. Chiniforoshan, Dalton Trans. 46 (2017) 14164–14173.
7. M.H. Abraham, N. Benjelloun-Dakhama, J.M.R. Gola, W.E. Acree Jr., W.S. Cain, J.E. Cometto-Muniz, New J. Chem. 24 (2000) 825–829.
8. L.V. Snegur, V.N. Babin, A.A. Simenel, Yu.S. Nekrasov, L.A. Ostrovskaya, N.S. Sergeeva, Russ. Chem. Bull., Int. Ed., 59 (2010) 2167–2178.
9. B.Ya. Andreev, L.M. Dyagileva, G.I. Feklisov, Dokl. Akad. Nauk. SSSR, 158 (1964) 1348–1351.
10. T. Noyhouzer, C. L'Homme, I. Beaulieu, S. Mazurkiewicz, S. Kuss, H.-B. Kraatz, S. Canesi, J. Mauzeroll, Langmuir 32 (2016) 4169–4178.
11. S.M. Batterjee, M.I. Marzouk, M.E. Aazab, M.A. El-Hashash, Appl. Organomet. Chem. 17 (2003) 291–297.
12. F.A. Larik, A. Saeed, T.A. Fattah, U. Muqadar, P.A. Channar, Appl. Organomet. Chem. 31 (2017) 3664.

13. G. Singh, A. Arora, S. Rani, I.K. Maurya, D. Aulakh, M. Wriedt, RSC Adv. 6 (2016) 82057–82081.

14. G. Singh, A. Arora, S. Rani, P. Kalra, D. Aulakh, M. Wriedt, Appl. Organomet. Chem. 31 (2017) 3728.

15. J.K. Puri, R. Singh, V.K. Chahal, Chem. Soc. Rev. 40 (2011) 1791–1840.

16. J. Huo, H. Hu, M. Zhang, X. Hu, M. Chen, D. Chen, J. Liu, G. Xiao, Y. Wang, Z. Wen, RSC Adv. 7 (2017) 2281–2287.

17. B. Schulze, U.S. Schubert, Chem. Soc. Rev. 43 (2014) 2522–2571.

18. S.N. Malkowski, C.F. Dishuck, G.G. Lamanilao, C.P. Embry, C.S. Grubb, M. Cafiero, L.W. Peterson, Molecules 22 (2017) 1682.

19. S.K. Mamidvala, M.G. Finn, Chem. Soc. Rev. 39 (2010)1252–1261.

20. T. Efthymiou, W. Gong, J.-P. Desaulniers, Molecules 17 (2012) 12665–12703.

21. H.C. Kolb, M.G. Finn, K.B. Sharpless, Angew. Chem. Int. Ed. 40 (2001) 2004–2021.

22. D. Coskun, M. Erkisa, E. Ulukaya, M.F. Coskun, F. Ari, Eur. J. Med. Chem. 136 (2017) 212–222.

23. P.S. Bhale, H.V. Chavan, S.B. Dongare, S.N. Shringare, Y.B. Mule, S.S. Nagne, B.P. Bandgar, Bioorg. Med. Chem. Lett. 27 (2017) 1502–1507.

24. M.N. Gomes, R.C. Braga, E.M. Grzelak, B.J. Neves, E. Muratov, R. Ma, L.L. Klein, S. Cho, G.R. Oliveira, S.G. Franzblau, C.H. Andrade, Eur. J. Med. Chem. 137 (2017) 126–138.

25. X. Gan, D. Hu, Z. Chen, Y. Wang, B. Song, Bioorg. Med. Chem. Lett. 27 (2017) 4298–4301.

26. A. Singh, J. Gut, P.J. Rosenthal, V. Kumar, Eur. J. Med. Chem. 125 (2017) 269–277.

27. H. Parveen, R.A.S. Alatawi, M.A. Alsharif, M.I. Alahmdi, S. Mukhtar, S.A. Khan, S. Hasan, A.U. Khan, Appl. Organomet. Chem. 2018, doi 10.1002/aoc.4257.

28. K. Kumar, B. Pradines, M. Madamet, R. Amalvict, V. Kumar, Eur. J. Med. Chem. 86 (2014) 113–121.

29. K. Kumar, S. Carrére-Kremer, L. Kremer, Y. Guérardel, C. Biot, V. Kumar, Organometallics 32 (2013) 5713–5719.

30. G. Singh, A. Arora, S.S. Mangat, S. Rani, H. Kaur, K. Goyal, R. Sehgal, I.K. Maurya, R. Tewari, D. Choquesillo-Lazarte, S. Sahoo, N. Kaur, Eur. J. Med. Chem. 108 (2016) 287–300.

31. A. Kamal, S.M.A. Hussaini, S. Faazil, Y. Poornachandra, G.N. Reddy, C.G. Kumar, V.S. Rajput, C. Rani, R. Sharma, I.A. Khan, N.J. Babu, Bioorg. Med. Chem. Lett. 23 (2013) 6842–6846.

32. R.J. Worthington, C. Melander, Trends Biotechnol. 31 (2013) 177–184.

33. G. Hernández-Alcántara, A. Torres-Larios, S. Enríquez-Flores, I. García-Torres, A. Castillo-Villanueva, S.T. Méndez, I. de la Mora-de la Mora, S. Gómez-Manzo, A. Torres-Arroyo, G. López-Velázquez, H. Reyes-Vivas, J. Oria-Hernández, PLoS One 8 (2013) 1–11.

34. U. Ryan, S.M. Cacciò, Int. J. Parasitol. 43 (2013) 943–956.

35. S.L. Cudmore, G.E. Garber, J. Infect. Public Health 3 (2010) 47–53.

36. S.L. Gottlieb, C.D. Deal, B. Giersing, H. Rees, G. Bolan, C. Johnston, P. Timms, S.D. Gray-Owen, A.E. Jerse, C.E. Cameron, V.S. Moorthy, J. Kiarie, N. Broutet, Vaccine 34 (2016) 2939–2947.

37. S.L. Gottlieb, N. Low, L.M. Newman, G. Bolan, M. Kamb, N. Broutet, Vaccine 32 (2014) 1527–1535.

38. I. Gülçin, Z. Huyut, M. Elmastaş, H.Y. Aboul-Enein, Arab. J. Chem. 3 (2010) 43–53.

39. G. Nabi, Z.-Q. Liu, Bioorg. Med. Chem. Lett. 21 (2011) 944–946.

40. N. Chavain, H. Vezin, D. Dive, N. Touati, J.-F. Paul, E. Buisine, C. Biot, Mol. Pharm. 5 (2008) 710–716.

41. A. Bianc, M. Maggini, M. Nogarole and G. Scorrano, Eur. J. Org. Chem. 13 (2006) 2934–2941.

42. G. Singh, A. Arora, S. Rani, P. Kalra, M. Kumar, Chemistry Select 2 (2017) 3637–3647.

43. M.B. Arnao, A. Cano, M. Acosta, Free Radic. Res. 31 (1999) 389–396.

44. J.F. Chen, Z.Q. Liu Liu, Chem. Res. Toxicol. 28 (2015) 451–459.

45. Y.F. Li, Z.Q. Liu, Eur. J. Pharm. Sci. 44 (2011) 158–163.

GRAPHICAL ABSTRACT

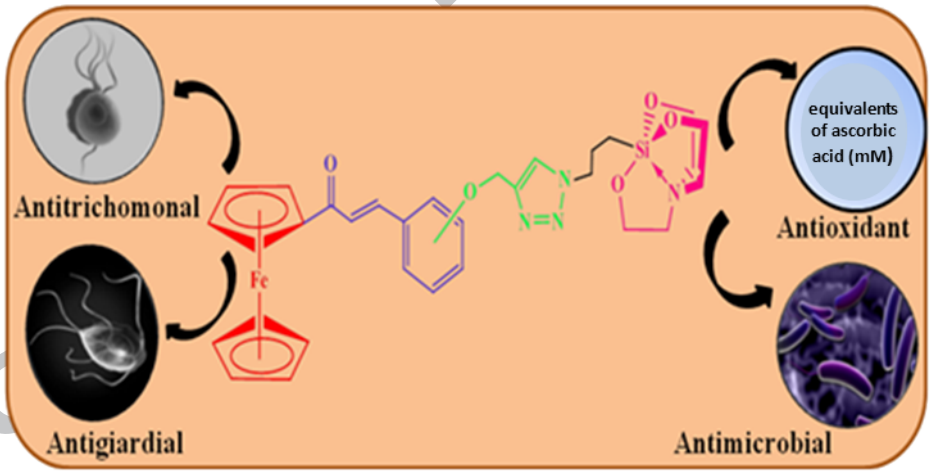

46.